Available online at www.elixirpublishers.com (Elixir International Journal)

Vibrational Spectroscopy

Elixir Vib. Spec. 91 (2016) 38577-38585

ISSN: 2229-712X

Density Functional Theory, Comparative Vibrational Spectroscopic Studies, NBO, HOMO–LUMO Analyses and Thermodynamic Functions of 3, 5 Dihydroxynaphthalene-2-carboxylicacid

B. Raja[1], V. Balachandran[2,*], B. Narayana[3] and B.Revathi[2]

[1]Department of Physics, Government Arts College, Kulithalai 639120, Karur, India.

[2]Department of Physics, A. A. Government Arts College, Musiri 621211, India.

[3]Department of Studies in Chemistry, University of Mangalore, Mangalagangotri 574 199, India.

ARTICLE INFO

Article history:

Received: 25 January 2016;

Received in revised form:

20 February 2016;

Accepted: 25 February 2016;

Keywords

DFT,

3, 5 Dihydroxynaphthalene-2-carboxylicacid,

Vibrational Spectra,

Mulliken Atomic Charges,

NBO,

HOMO-LUMO Energy Gap,

MEP Surface.

ABSTRACT

Fourier transform infrared and Fourier transform Raman spectra of 3, 5 dihydroxynaphthalene-2-carboxylicacidwere recorded in the regions 4000–450 cm^{-1} and 3500–100cm^{-1}, respectively in the solid phase. The vibrational frequencies were calculated by density functional B3LYP methods with ccPVDZ and 6-31+G(d) basis sets, using Gaussian 09W program package. A detailed interpretation of the infrared and Raman spectra of 3, 5 dihydroxynaphthalene-2-carboxylicacid is reported. The thermodynamic functions of the title compound were also studied by the above methods and the basis set. The stability of the molecule arising from hyper conjugative interactions and accompanying charge delocalization has been analyzed using natural bond orbital (NBO) analysis. The HOMO and LUMO energy gap reflects the chemical activity of the molecule. The observed and calculated wave numbers are found to be in good agreement.

Introduction

Vibrational spectroscopy is used extensively in organic chemistry, for the identification of functional groups of organic compounds, for studies on molecular conformation, reaction kinetics, etc. [1]. Due to the great biochemical importance the vibrational spectral studies of Naphthoic acid (NA) have been carried out in the present investigation. Naphthalene and its derivatives are biologically, pharmaceutically and industrially useful compounds. 2-Acetonaphthalene provides the best raw material for the preparation of 2-naphthoic acid. The structure of naphthalene is benzene-like, having two–six membered rings fused together. Particularly, naphthalene was studied because, of its technological applications in a vast amount of industrial process. In fact, it was used as a precursor for the synthesis of plastics and dyes, gamma-ray detector in photo-multiplier tubes and also used in dye stuffs, synthetic resins, coatings, tanning agent and celluloid [2].

Though the lower acids like formic and acetic acids have been extensively studied only few studies exist for the higher acids. Quantum chemical calculations involving carboxylic acids have to account for the electron rich carboxyl group. Modern vibrational spectrometry has proven to be an exceptionally powerful technique for solving many chemical problems. It has been extensively employed both in the study of chemical kinetics and chemical analysis. The problem of signal assignment however, as well as understanding the relationship between the observed spectral features and molecular structure, and reactivity can be difficult. Even identification of fundamental vibrational frequencies often generates controversy. FT-IR, FT-Raman spectroscopy combined with quantum chemical computations have been recently used as an effective tool in the vibrational analysis of drug molecules [3], biological compounds [4] and natural products [5], since fluorescence-free Raman spectra and the computed results can help unambiguous identification of vibrational modes as well as the bonding and structural features of complex organic molecular systems. The present work deals with density functional theoretical (DFT) computations and vibrational spectral analysis of 3,5dHN2CA.

Experimental Details

3,5dHN2CA was provided by Lancaster Chemical Company, UK. Which is of spectroscopic grade and hence used for recording the spectra as such without any further purifications. The room temperature Fourier Transform infrared spectrum of 3,5dHN2CA was measured in the 4000-450 cm^{-1}region at a resolution of ± 1 cm^{-1} using BRUKER IFS-66V FT-IR Spectrometer equipped with a KBR pellets were used in the spectral measurements. The FT-Raman spectrum was recorded on a BRUKER IFS-66V model interferometer equipped with an FRA -106 FT-Raman accessories in the 3500-100 cm^{-1}stokes region using the 1064nm line of an Nd: YAG laser for excitation operating at 200mW Power. The reported wave numbers are expected to be accurate within ± 1 cm^{-1}

Tele: +91 9894253672

E-mail address: brsbala@rediffmail.com

Computational details

Analysis of molecular geometry optimizations, energy, and vibrational frequencies was carried out with the Gaussian 09 software package [6] at the DFT (B3LYP) levels supplemented with the standard ccPVDZ and 6-31+G(d)basis sets. Cartesian representation of the theoretical force constants has been computed at optimized geometry. Vibrational Modes were assigned by means of visual inspection using the GAUSSVIEW [7] program. Data revealed that DFT calculations using a basis set incorporating polarized functions yielded results that are in better agreement with the experimental data. For the plots of simulated IR and Raman spectra, pure Lorentzian band shapes were used with a band width of ±1 cm^{-1}. Prediction of Raman intensities was carried out by the following procedure. The Raman activities (Si) calculated by the Gaussian 09 program were converted to relative Raman intensities (Ii) using the following relationship derived from the basic theory of scattering.

$$I_i = \frac{f(\nu_0 - \nu_i)^4 s_i}{\nu_i[1 - \exp(\frac{-hc\nu_i}{kt})]}$$

Where ν_0 is the exciting wave number (cm^{-1} units ν_i is the vibrational wave number of the i^{th} normal mode, h, c and k are universal constant and f is a suitably chosen common normalization factor for all peak intensities.

Results and discussion

Molecular geometry

The molecular structure of a 3,5dHN2CA along with numbering of atoms is shown in Fig.1. The maximum number of potentially active observable fundamentals of a non-liner molecule that contains N atoms is equal to (3n-6), apart from three translational and three rotational degrees of freedom [8]. 3,5dHN2CA having 23 atoms with 63 Normal modes of vibrations which are distributed amongst the symmetry species as $(3N-6)_{vib}$=43A' (in-plane) + 20" (out-of-plane). The A' vibrations are totally symmetric and give rise to polarized Raman lines whereas A" vibrations are antisymmetric and give rise to depolarized Raman lines. Figs.2 and 3 shows the observed and calculated B3LYP/ccPVDZ and B3LYP/6-31+G(d)FT-IR and FT-Raman spectra of 3,5dHN2CA , respectively.

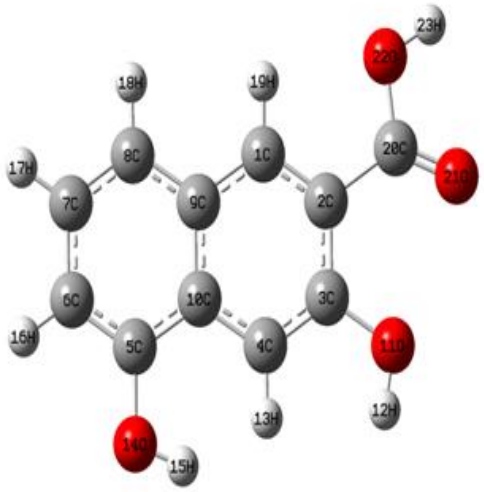

Fig 1. Optimized geometrical structure and atomic labeling of 3,5dihydroxynaphthalene-2-Carboxylicacid

The most optimized geometrical parameters (bond length and bond angle) were calculated by B3LYP/ccPVDZ and B3LYP/6-31+G(d)basis sets, which are depicted in Table 1.

Vibrational Assignments

The detailed vibrational analysis of fundamental modes of 3,5dHN2CA along with the FT-IR and FT-Raman experimental frequencies and the unscaled and scaled vibrational frequencies using B3LYP/ccPVDZ and B3LYP/6-31+G(d)basis sets are presented in Table 2.

CH vibrations

The existence of one or more aromatic rings in a structure is normally readily determined from the C−H and C=C−C ring related vibrations. The C−H stretching occurs above 3000 cm^{-1} and is typically exhibited as a multiplicity of weak to moderate bands, compared with the aliphatic C−H stretch [9]. These vibrations are not found to be affected by the nature and position of the substituents. In the present work, the C−H stretching vibration is observed in the FT-IR spectrum at 3068, 3027, 2998cm^{-1} and in the FT-Raman spectrum at 3070, 3050, 3000, 2975cm^{-1}.The vibration is calculated in the range 3070–2972cm^{-1} by theB3LYP/6-31+G(d) method and this shows good correlation with the experimental data. As indicated by the TED, these modes(mode Nos. 4–8) involve more than 96% of contribution suggesting that they are pure stretching modes. All the aromatic C−Hstretching bands are found to be weak and this is due to the decrease of dipole moment caused by the reduction of negative charge on the carbon atom. This reduction occurs because of the electron withdrawal from the carbon atom by the substituent due to the decrease of inductive effect, which in turn is causedby the increased chain length of the substituent [10].

The aromatic C−H in-plane bending vibrations of benzene and its derivatives are observed in the region 1300–1000 cm^{-1}[11].The bands are sharp and of weak to very strong intensity. In accordance with the above literature data, were observed in the FT−IR spectrum at1056, 1016, 962, 930, 908$cm^{-1}$and FT−Raman spectrum at1018, 926 $cm^{-1}$are assignedto C−H in-plane bending vibrations. This shows good agreement with the theoretically computed results B3LYP/6-31+G(d)method.

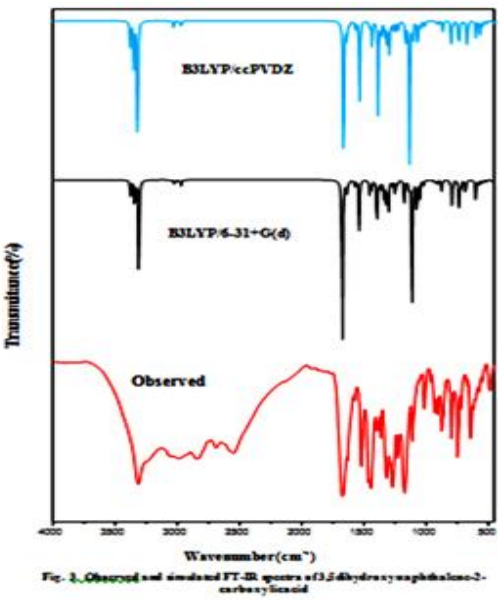

Fig. 2. Observed and simulated FT-IR spectra of 3,5dihydroxynaphthalene-2-carboxylicacid

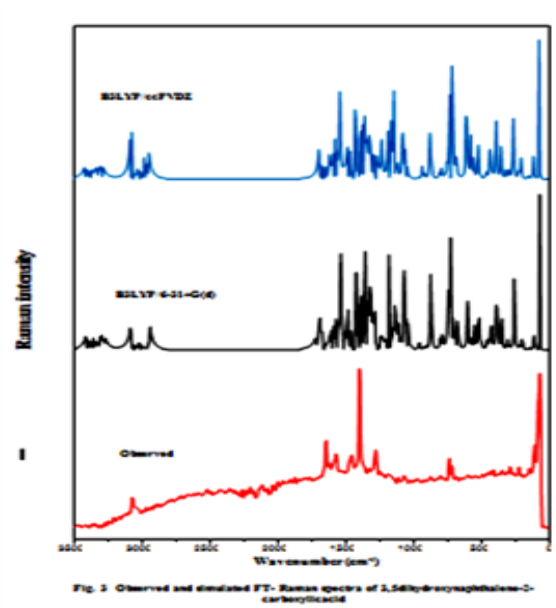

Table 1. Optimized geometrical parameters of 3, 5 dihydroxynaphthalene-2-carboxylicacid by B3LYP/ccPVdZ and B3LYP/6-31+G(d).

Parameters	Bond length		Parameters	Bond angle	
	B3LYP/ ccPVDZ	B3LYP/6-31+G(d)		B3LYP/ ccPVDZ	B3LYP/6-31+G(d)
C1-C2	1.39	1.39	C2-C1-C9	121.77	121.90
C1-C9	1.41	1.41	C2-C1-H19	118.93	119.00
C1-H19	1.09	1.09	C9-C1-H19	119.30	119.10
C2-C3	1.44	1.44	C1-C2-C3	119.95	119.55
C2-C20	1.47	1.47	C1-C2-C20	121.34	121.10
C3-C4	1.39	1.38	C3-C2-C20	118.71	119.35
C3-O11	1.35	1.35	C2-C3-C4	119.14	119.52
C4-C10	1.41	1.41	C2-C3-O11	121.92	122.29
C4-H13	1.09	1.08	C4-C3-O11	118.94	118.19
C5-C6	1.38	1.38	C3-C4-C10	120.97	120.90
C5-C10	1.43	1.43	C3-C4-H13	118.78	118.79
C5-H14	1.37	1.37	C10-4-H13	120.25	120.31
C6-C7	1.42	1.42	C6-C5-C10	120.62	120.86
C6-16	1.09	1.09	C6-C5-O14	123.41	123.20
C7-C8	1.37	1.37	C10-C5-O14	115.97	115.94
C7-H17	1.09	1.09	C5-C6-C7	120.75	120.64
C8-C9	1.43	1.43	C5-C6-H16	119.57	119.82
C8-H18	1.09	1.09	C7-C6-H16	119.68	119.55
C9-C10	1.44	1.44	C6-C7-C8	120.52	120.50
O11-H12	0.99	0.98	C6-C7-H17	119.00	119.00
O14-H15	0.97	0.97	C8-C7-H17	120.48	120.50
C20-O21	1.23	1.23	C7-C8-C9	120.09	120.06
C20-O22	1.35	1.35	C7-C8-H18	120.93	120.89
O22-H23	0.97	0.98	C9-C8-H18	118.98	119.05
			C1-C9-C8	122.12	121.96
			C1-C9-C10	117.80	117.90
			C8-C9-C10	120.08	120.14
			C4-C10-C5	121.68	121.97
			C4-C10-C9	120.37	120.23
			C5-C10-C9	117.95	117.80
			C3-O11-H12	106.92	108.44
			C5-O14-H15	108.75	109.84
			C2-C20-O21	124.45	124.58
			C2-C20-O22	114.83	114.85
			O21-O20-O22	120.71	120.57
			O20-O22-H23	105.77	106.72

Moreover, the substitution patterns on the ring can be judged from the out of plane bending of the C−H bonds, which appear in the region 900–675 cm^{-1}[12]. The bands observed at 459cm^{-1} in the FT-IR spectrum and the medium strong to very weak bands observed at 600, 500, 454 and 413cm^{-1} in the FT-Raman spectrum are assigned to C−H out-of-plane bending vibrations in 3,5dHN2CA. The theoretically computed wave number for this mode falls within the range at 601,501, 458, 432 and415cm^{-1} by the both of B3LYP/cc PVDZ and B3LYP/6-31+G(d) methods.

CC and ring vibrations

The ring stretching vibrations are very much important in the spectrum of Naphthalene derivatives and are highly characteristic of the aromatic ring itself. However, empirical assignments of vibrational modes for peaks in the fingerprint region are not easy. Sathyanarayana [13] noted that the bands 1430–1650 cm^{-1}were due to C−Hstretching modes. Socrates [14] noted that the presence of conjugate substituents like C=C causes a heavy doublet formation around the region 1625–1575 cm^{-1}. The six ring carbon atoms undergo coupled vibrations called skeletal vibrations and give a maximum of four bands in the region 1660–1420 cm^{-1}[15]. As predicted in the earlier references, in the present work, the C−Haromatic stretch is observed at 1639, 1574, 1441, 1398, 1377, 1273and 1229cm^{-1} in the FT-IR spectrum and at 1642, 1621, 1572, 1538, 1399, 1338, 1277, 1250, and 1225 cm^{-1} in the FT-Raman spectrum. These vibrations are in agreement with the scaled theoretical assignments given by DFT.

OH vibrations

The hydroxyl stretching vibrations are generally [16,17] observed in the region around 3500 cm^{-1}. The peak is broader and its intensity is higher than that of a free O−H vibration, which indicates the involvement in an intramolecular hydrogen bond. A computed values of 3383 and 3316cm^{-1} have been assigned to the (OH) stretching frequencies in B3LYP method whereas the experimentally observed frequencies are 3315$cm^{-1}$are found in FT-IR spectrum. The in-plane O−H deformation vibration usually appears as strong band in the region 1440–1260 cm^{-1} in the spectrum, which gets shifted to lower wavenumber in the presence of hydrogen bonding. The strong band at 1173 and 1112cm^{-1} correspond to the O−H in-plane bending mode that is coupled to ring stretching vibration of the benzene ring in FT-IR spectrum. The O−H out-of-plane bending vibrations give rise to a broad band in the region 700–600 cm^{-1}. Computational data for OH out-of-plane bending are obtained at 605, 551 cm^{-1} whereas experimentally, observed value are at 602 and 550 cm^{-1}in IR spectrum. The computed wavenumbers are in good agreement with the experimental and literature values [18,19].

COOH vibrations

The carboxylic acid O−H stretching bands are weak in the Raman spectrum, so IR data are generally used. The O−H stretching is characterized by a very broad band appearing near about 3400 cm^{-1}[20]. On the other hand, the hydrogen bonding in the condensed phase with the other acid molecules makes vibrational spectra more complicated. Therefore, we could not observe the strong and sharp bands of the OH vibration in the IR and Raman spectra. However, this band is calculated at 3353cm^{-1}, the PED corresponds to this vibration is exactly pure one contributing to 99%.

The most characteristic feature of carboxylic group is a single sharp and observed usually in the range of 1690–1655 cm^{-1}[21] due to the C=O stretching vibration.

Table 2. Vibrational assignments of fundamental observed frequencies and calculated frequencies of 3,5dihydroxynaphthalene-2-carboxylic acid by B3LYP/ccPVdZ and B3LYP/6-31+G(d).

Mode No.	Symmetry species	Observed frequencies		Calculated frequencies				Infrared intensities		Raman intensities		Vibrational assignments / (%)
		FT-IR	FT-Raman	Unscaled		Scaled						
				B3LYP/ ccPVDZ	B3LYP/ 6-31+G(d)	B3LYP/ ccPVDZ	B3LYP/ 6-31+G(d)	B3LYP/ ccPVDZ	B3LYP/ 6-31+G(d)	B3LYP/ ccPVDZ	B3LYP/ 6-31+G(d)	
1	A’			3782	3759	3380	3383	70.46	63.82	49.47	48.58	υOH(100)
2	A’			3716	3696	3353	3350	120.46	115.25	57.66	48.11	υOH(100)
3	A’	3315		3401	3473	3322	3316	420.54	363.77	59.52	59.48	υOH(99)
4	A’	3068	3070	3230	3239	3070	3068	1.56	1.71	40.37	37.72	υCH(99)
5	A’		3050	3208	3219	3057	3053	1.54	1.45	34.93	30.93	υCH(98)
6	A’	3027		3200	3208	3032	3028	18.46	21.31	11.19	10.74	υCH(98)
7	A’	2998	3000	3180	3189	2994	2998	4.28	5.30	30.14	27.97	υCH(98)
8	A’		2975	3158	3168	2972	2976	20.35	21.50	31.09	38.78	υCH(97)
9	A’	1673		1753	1742	1670	1675	518.98	651.66	44.39	45.38	υC=O(62), υCC(10), υOH(12)
10	A’	1639	1642	1685	1682	1643	1640	52.51	49.47	27.00	26.25	υCC(57), υCO(18), υOH(18)
11	A’		1621	1658	1655	1625	1626	9.64	11.43	19.82	23.65	υCC(63), υCO(18), υOH(9)
12	A’	1574	1572	1621	1616	1575	1575	20.79	19.51	38.62	31.95	υCC(69), υOH(27)
13	A’		1538	1567	1563	1540	1539	208.89	176.08	25.13	24.72	υCC(67), υOH(21)
14	A’		1455	1502	1503	1460	1456	22.60	47.11	74.21	68.26	υCO(63), υCH(18), υOH(14)
15	A’	1441		1494	1499	1443	1440	69.69	38.55	37.39	31.87	υCC(54), υOH(17), υCH(9)
16	A’	1398	1399	1457	1444	1393	1396	246.05	196.20	22.15	26.18	υCC(69), υCH(24), υOH(11)
17	A’	1377		1439	1435	1379	1378	2.18	4.82	13.60	17.25	υCC(68), υOH(24)
18	A’	1365		1415	1408	1367	1366	42.38	28.41	13.82	10.53	υCO(59), υOH(27)
19	A’		1338	1399	1394	1339	1340	45.74	91.81	8.74	5.67	υCC(61), υOH(18), υCH(9)
20	A’	1317		1349	1339	1320	1320	89.62	112.26	18.17	23.56	υCO(72), υOH(27)
21	A’’			1307	1310	1301	1302	88.27	97.37	14.99	5.47	υCC(69), υCH(14), υOH(10)
22	A’	1273	1277	1281	1278	1277	1275	32.97	17.20	55.25	48.16	υCC(73), υCO(18)
23	A’		1250	1253	1264	1252	1250	27.14	65.80	3.79	4.19	υCC(77), υCH(17)
24	V	1229	1225	1246	1255	1230	1230	29.16	16.31	20.41	20.40	υCC(70), υCH(16)
25	A’	1173		1206	1206	1172	1175	80.69	77.09	24.10	27.49	δOH (71), δCH (18)
26	A’		1138	1180	1194	1140	1138	396.23	43.87	20.28	22.72	δOH (81), δCH (11)
27	A’	1112	1114	1171	1183	1114	1113	46.59	398.43	6.14	28.21	δOH (81), δCH (8)
28	A’	1076	1074	1111	1115	1075	1075	83.00	140.65	37.15	31.12	δCC(73), δCH(19)
29	A’	1056		1079	1085	1052	1050	20.80	58.89	36.92	45.94	δCH(74), δCO(19)
30	A’	1016	1018	1034	1032	1019	1020	21.60	22.10	0.50	1.01	δCH(77), δCC(11) δCO(7)
31	A’	962		973	967	963	962	1.17	3.03	0.63	0.38	δCH(88)
32	A’	930	926	940	934	932	928	4.94	13.20	2.20	1.86	δCH(82), δCC(12)
33	A’’	908		909	904	912	910	12.01	13.66	1.37	1.80	δCH(81), δCC(14)
34	A’		874	883	885	876	875	30.27	35.76	31.38	34.13	$\delta R2_{trigd,}$(68)
35	A’	863		873	873	865	865	1.92	5.18	15.50	6.56	$\delta R2_{asym,}$(69)
36	A’		804	818	807	806	806	62.35	12.16	3.79	6.08	δCO(59), δCH(28)
37	A’	791		809	795	790	790	10.26	88.16	7.57	8.97	$\delta R1_{trigd,}$(58)
38	A’	747		807	781	750	747	33.61	2.56	8.52	11.51	$\delta R1_{asym,}$(69)
39	A’		736	760	737	740	735	56.71	87.07	0.30	5.13	δCO(69), δOH(24)
40	A’			752	733	729	730	0.01	2.69	43.56	33.06	$\delta R2_{asym,}$(58)
41	A’	718	718	733	731	715	719	3.40	32.34	1.32	1.35	$\delta R1_{sym,}$(57)
42	A’		688	713	711	680	683	63.19	58.67	17.41	19.45	δCO(58), δOH(21)
43	A’	671		696	684	670	670	14.41	4.11	0.00	11.59	δCO(51), δOH(21), δCC(12)
44	A’’	602		609	603	608	605	47.08	0.02	63.35	45.97	γ OH(74), γ δCH(23)
45	A’’		600	601	602	601	600	0.17	80.13	49.18	21.99	γ CH(58), δCO(21)
46	A’’	574		585	584	575	575	38.28	16.18	54.69	10.89	γ OH(57), γ δCH(17)
47	A’’	550		584	583	552	551	14.62	14.87	24.98	31.76	γ OH(67), δCH(14)
48	A’’	519		556	557	520	520	9.90	10.05	62.65	75.75	$\gamma R2_{trigd}$(65)
49	A’’		500	548	539	501	501	0.01	0.28	4.05	10.85	γ CH(67),δCO(17)
50	A’’	459	454	468	468	458	458	10.79	13.01	15.38	19.82	γ CH(64),δCO(14)
51	A’’			445	445	431	432	0.59	0.90	83.16	95.63	γ CH(62),δCC(11)
52	A’’		413	440	438	415	415	2.73	7.83	10.20	12.00	γ CH(62), δOH(28)
53	A’’			406	406	387	388	3.07	3.85	82.05	93.50	γ CC(59), δCH(18)
54	A’’		347	376	367	350	352	80.72	95.83	93.01	96.23	$\gamma R1_{trigd}$(65)
55	A’’		313	345	348	315	310	8.80	7.39	24.11	30.87	$\gamma R1_{asym}$(67)
56	A’’		290	338	334	292	293	25.16	20.78	43.03	9.04	$\gamma R2_{sym}$(63),
57	A’’		261	262	262	260	258	3.97	3.92	40.99	42.85	$\gamma R1_{sym}$(65)
58	A’’		224	247	243	220	221	0.01	0.00	49.81	53.99	$\gamma 2_{asym}$(68)
59	A’’		200	216	211	203	200	0.96	1.35	26.15	32.52	γ CO(54),δCC(17)
60	A’’		149	179	179	150	150	1.37	1.48	15.81	16.58	γ CO(63)
61	A”		109	127	122	112	110	0.64	0.86	69.97	60.48	γ CO(57), γ CH(16)
62	A”		71	90	84	72	70	0.55	0.61	20.88	29.07	γ Ring Butterfly(59)
63	A”			70	68	63	65	0.94	0.59	11.33	10.58	γ CO(48), γ CC(12)

A’: In-plane; A”: out-of-plane; sym: symmetric stretching; asym: asymmetric stretching; υ:stretching;δ: in-plane bending; γ: out-of-plane bending; t: torsion; wagg: wagging; sciss:scissoring; τ: twisting; sb: symmetric bending; ipb: in- plane-bending; opb: out-plane-bending; ipr:in-plane-rocking;opr: out-plane-rocking;

The C−O stretching vibration is normally observed at 1320–1210 cm^{-1} due to C−O stretching vibrations [22]. The C=O and C−O stretching vibrations are observed at 1673, 1365and 1317cm^{-1} respectively, for the present molecule. The C=O vibrational band is observed in the end of the expected range and C−O stretching is slightly deviated to lower wavenumber side. The C−O in-plane bending bands are found at 671cm^{-1} in FT-IR and 804, 736, 688 cm^{-1} in FT-Raman and the calculated B3LYP wavenumber at 806,735, 683 and 670cm^{-1}, and the C−O out-of plane bending bands are calculated B3LYP wavenumber at 200 cm^{-1},respectively. This view also supported by the above literature.

A very strong band is observed at 1138cm^{-1} in FT-Raman spectrum is assigned to O–H in-plane bending. The observed strong band at 574cm^{-1}in FT-IR is O−H out-of-plane vibration is assigned. According to the literature [23,24], both the bending vibrations are moved down slightly by the mixing of the ring CC vibration is found with very strong intensity at 1398cm^{-1}in IR which clearly indicates that its dipole bond character. The very strong absorption bands at 1398cm^{-1} in FT-IR and at 1399cm^{-1}in FT-Raman spectra correspond to C−COOH stretching vibration. The C−COOH in-plane and out-of-plane bending vibrations are identified at 1075 and 388cm^{-1}. The above results are in good agreement with earlier work [25]. The PED of these modes are mixed one as it is shown in Table 2.

Natural bond orbital analysis

Natural bond analysis gives the accurate possible natural Lewis structure picture of φ because all orbital mathematically chosen to include the highest possible percentage of the electron density. Interaction between both filled and virtual orbital spices information correctly explained by the NBO analysis, it could enhance the analysis of intra- and intermolecular interactions. The second order Fock matrix was carried out to evaluate donor (i) acceptor (j) i.e. donor level bonds to acceptor level bonds interaction in the NBO analysis [26]. The result of interaction is a loss of occupancy from the concentrations of electron NBO of the idealized Lewis structure into an empty non-Lewise orbital. For each donor (i) and acceptor (j), the stabilization energy E(2) associates with the delocalization i→j is estimated as,

$$E_2 = \Delta E_{ij} = q_i \frac{F^2(i,j)}{\varepsilon_j - \varepsilon_i}$$

where q_i is the donor orbital occupancy, are ε_j and ε_i diagonal elements and F(i, j) is the off diagonal NBO Fock matrix element. Natural bond orbital analysis is used for investigating charge transfer or conjugative interaction in the molecular system. Some electron donor orbital, acceptor orbital and the interacting stabilization energy resulted from the second-order micro-disturbance theory are reported [27, 28]. The larger E(2), value the more intensive is the interaction between electron donor and acceptor, i.e. the more donation tendency from electron donors to electron acceptors and the greater the extent of conjugation of the whole system [29]. Delocalization of electron density between occupied Lewis-type (bond or lone pair) NBO orbitals and formally unoccupied (antibond or Rydberg) non-Lewis NBO orbitals correspond to a stabilization donor–acceptor interaction.NBO analysis has been performed of the title molecule at the DFT/B3LYP/6- 31+G(d) level in order to elucidate the intramolecular, rehybridization and delocalization of electron density within the molecule.

The intramolecular interaction is formed by the orbital overlap between σ (C1–C19), σ (C2–C20), σ (C3–O11),σ (C5–O14) and σ*(C2–C3), σ*(C22–H23), σ*(C1–C2), σ*(C9–C10) bond orbital, which results intramolecular charge transfer causing stabilization of the system. The most important interactions in the title molecule having lone pair O22(1) with that of antibonding π*(C20–O21),lone pair O11(2) with that of antibonding π*(C3–C4) and the lone pair O22(2) with that of antibonding π*(C20–O21) results the stabilization of 6.82, 24.02kJ mol^{-1} and 45.56 kJ mol^{-1}, respectively, which donates larger delocalization. The maximum energy transfer occurs from LPO22(1) and LPO22(2) to σ*(C20–O21) and π* (C20–O21) as shown in Table 4. The ED inO22(2) and O11(2) lone pairs are moderates increased the electron density of π*(C20–O21) and σ*(C20–O21) are of 0.26173e and0.29243e, respectively, which yields to weakening the bond and its elongation from the ring carbon atoms of the title molecule.

Frontier molecular orbital's (FMOs) and atomic charges

The most important orbital's in molecule is the frontier molecular orbital's, called highest occupied molecular orbital (HOMO) and lowest unoccupied molecular orbital (LUMO). These orbitals determine the way the molecule interacts with other species. The frontier orbital gap helps to characterize the chemical reactivity and kinetic stability of the molecule. A molecule with a small frontier orbital gap is more polarizable and is generally associated with a high chemical reactivity, low kinetic stability and is also termed as soft molecule [30]. The low values of frontier orbital gap in 3,5dHN2CA make it more reactive and less stable. The HOMO is the orbital that primarily acts as an electron donor and the LUMO is the orbital that largely acts as the electron acceptor. The 3D plot of the frontier orbital's HOMO and LUMO for 3,5dHN2CA molecule are shown in Fig. 4. The positive phase is red and the negative one is green (For interpretation of the references to color in this text, the reader is referred to the web version of the article).

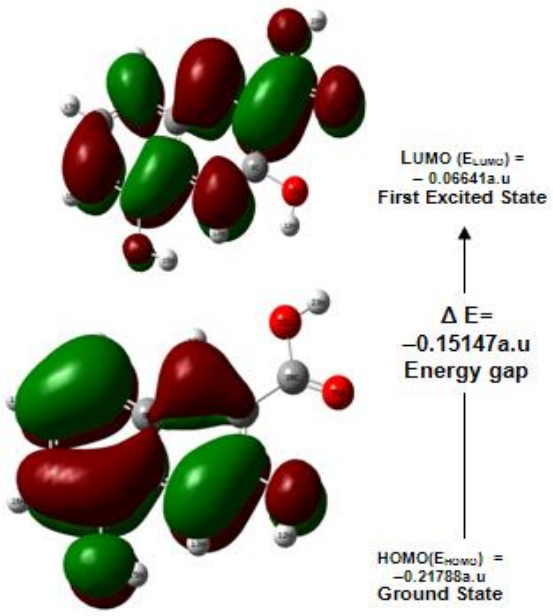

Fig 4. The atomic orbital composition of the molecular orbital for 3,5dihydroxynaphthalene-2-carboxylicacid

In most cases, even in the absence of inversion symmetry, the strongest band in the FT-Raman spectrum is weak in the FT-IR spectrum vice versa. But the intra-molecular charge transfer from the donor to acceptor group through a single-double bond conjugated path can induce large variations of both the molecular dipole moment and the molecular polarizability, making FTIR and FT-Raman activity strong at the same time. The experimental spectroscopic behavior described above is well accounted by ab initio calculations in p conjugated systems that predict exceptionally large Raman and IR intensities for the same normal modes [31]. It is also observed in our title molecule the bands in FTIR spectrum have their counterparts in FT-Raman shows that the relative intensities in FTIR and FT- Raman spectra are comparable resulting from the electron cloud movement through π conjugated frame work from the electron donor to electron acceptor groups. The analysis of the wave function indicates that the electron absorption corresponds to the transition from the ground to the first excited state and is mainly described by one-electron excitation from the highest occupied molecular orbital (HOMO) to the lowest unoccupied molecular orbital (LUMO). The HOMO of π nature, (i.e., benzene ring) is delocalized over the C-C bond. By contrast, LUMO is located over hydroxyl, and oxygen atoms of carboxylic acid group. It can be seen from the Fig. 4 that, the HOMO is distributed in ring and hydroxyl group of title molecule. The LUMO in C2-C20 and O21 of carboxylic acid group are found to spread over the ring. All the HOMO and LUMO have nodes. The nodes in each HOMO and LUMO are placed symmetrically.

The energy gap of HOMO–LUMO explains the eventual charge transfer interaction within the molecule, which influences the NLO activity of the molecule. As the energy gap between the LUMO and HOMO decreases, it is easier for the electrons of the HOMO to be excited. The higher the energy of HOMO, the easier it is for HOMO to donate electrons whereas it is easier for LUMO to accept electrons when the energy of LUMO is low. The energy values of HOMO and LUMO levels are computed to be -0.21788 a.u. and -0.06641 a.u., respectively, and the energy difference is 0.15147a.u.

The calculation of atomic charges plays a key role in the application of quantum mechanical calculation to describe the electronic characteristics of molecular systems [32]. A comparative study of the NBO and Mulliken atomic charge distributions in 3,5-diHydroxy naphthalene-2-carboxylicacid.determined on the basis of quantum mechanical method with B3LYP method is presented in Table 3.

Both Mulliken's atomic net charges [33–35] and the natural NBO/NPA atomic charges were calculated. The results are listed in Table 3. Regarding the molecular symmetries only the charges of 23 atoms are listed for title molecule. The comparison between Mulliken's net charges and the atomic natural one is not an easy task since the theoretical background of the two methods was very different. Looking at the results there are surprising differences between the Mulliken's and the NBO charges. All of the NBO charges have the negative sign for C1and C2 atom on the B3LYP method, whilst the Mulliken's values for the C1 atom have same sign and C2 atom are different in sign as compared to these values for the method.

The definition of Mulliken's charges is based on population analysis. The Mulliken population analysis provides a partitioning of either the total charge density or an orbital density. The number of electrons in molecule (N) is the integral of the charge density over the space. N is partitioned for all atoms considering also the overlap population. According to the theory the overlap population of atoms A and B is divided between the two atoms in half-to-half ratio. This is one weak point of the theory. The other weak point is its strong dependence on the basis set applied. The Mulliken's atomic net charges are presented in Table 3.

Table 3. The charge distribution calculated by the Mulliken and natural bond orbital (NBO) methods using DFT/B3LYP/6-31+G(d)of 3,5dihydroxynaphthalene-2-carboxylicacid molecule.

Atoms	DFT	
	Atomic charges(Mulliken)	Natural charges(NBO)
C1	-0.20827	-0.14469
C2	0.19909	-0.20956
C3	-0.35864	0.33961
C4	-0.77052	-0.25432
C5	0.38263	0.32484
C6	0.10033	-0.29524
C7	-0.55475	-0.23179
C8	-0.34203	-0.21626
C9	-0.34684	-0.07203
C10	0.69893	-0.07205
O11	-0.69750	-0.73755
H12	0.54510	0.53936
H13	0.22802	0.27450
O14	-0.70770	-0.71801
H15	0.50838	0.50678
H16	0.16622	0.23613
H17	0.18321	0.24497
H18	0.18369	0.24105
H19	0.22190	0.26305
C20	1.24239	0.81757
O21	-0.55817	-0.63459
O22	-0.63566	-0.72710
H23	0.52018	0.52533

Molecular electrostatic potentials (MEPs)

Molecular electrostatic used extensively for interpreting potentials have been and predicting the reactive behavior of a wide variety of chemical system in both electrophilic and nucleophilic reactions, the study of biological recognition processes and hydrogen bonding interactions [36]. V(r), at a given point r(x,y,z) in the vicinity of a compound, is defined in terms of the interaction energy between the electrical charge generated from the compound electrons and nuclei and positive test charge (a proton) located at r. Unlike, many of the other quantities used at present, and earlier as indices of reactivity V(r) is a real physical property that can be determined experimentally by diffraction or by computational methods. For the systems studied the MEP values were calculated as described previously, using the equation [37].

$$V(\mathrm{r}) = \sum \frac{Z_A}{|R_A - r|} - \int \frac{\rho(r')}{|r' - r|} dr$$

Where the summation runs over all the nuclei A in the compound and polarization and reorganization effects is neglected. Z_A is the charge of the nucleus A, located at R and q(r') is the electron density function of the compound.

To predict reactive sites for electrophilic and nucleophilic attack for the investigated compound, molecular electrostatic potential (MEP) was calculated at B3LYP/ccPVDZ optimized geometries. Red and blue areas in the MEP map refer to the electron-rich and electron-poor regions, respectively, whereas the green color signifies the neutral electrostatic potential. The

MEP surface provides necessary information about the reactive sites. The electron total density onto which the electrostatic potential surface has been mapped is shown in Fig. 5.

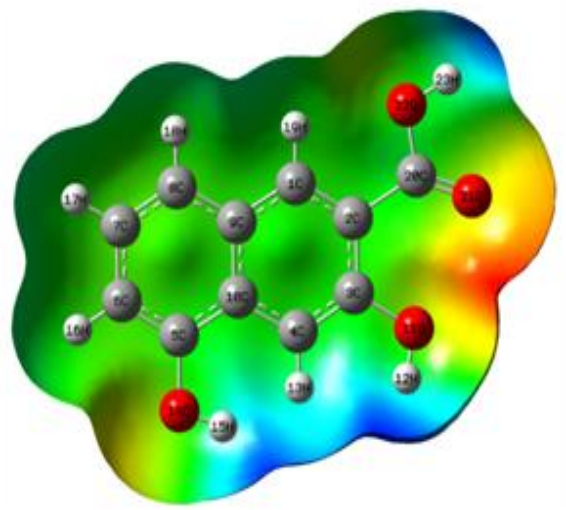

Fig 5. DFT (B3LYP)/6-31+G(D) calculated 3D molecular electrostatic potential of 3,5dihydroxynaphthalene-2-carboxylicacid

The negative regions V(r) were related to electrophilic reactivity and the positive ones to nucleophilic reactivity. As easily can be seen in Fig. 5, this compound has several possible sites for electrophilic attack in which V(r) calculations have provided in-sights. Thus, it would be predicted that an electrophile would preferentially attack 3,5dHN2CA at the oxygen atoms of carboxyl, and hydroxylic position.

Alternatively, we found the positive regions over the hydrogen atoms of 3,5dHN2CA compound and indicating that these sites can be the most probably involved in nucleophilic processes.

Thermodynamic properties

On the basis of vibrational analysis, the statically thermodynamic functions: heat capacity (Cp), enthalpy changes (ΔH), Gibb's free energy (Δ) and entropy (S^0m) for the title molecule were obtained from the theoretical harmonic frequencies and listed in Table 5. From the Table 5, it can be observed that these thermodynamic functions are increasing with temperature ranging from 100 to 1000 K due to the fact that the molecular vibrational intensities increase with temperature. The correlation equations between heat capacity, Gibb's free energy, entropy, enthalpy changes and temperatures were fitted by quadratic formulas and the corresponding fitting factors (R2) for these thermodynamic properties are 0.999, 0.999, 0.999 and 0.999, respectively. The corresponding fitting equations are as follows and the correlation graphics of those shown in Figs. 6.

$$\left(Cp^0\right) = 0177 + 19.03T - 0.869T^2 \left(R^2 = 0.999\right)$$

$$\left(S^0\right) = 54.91 + 15.11T + 0.270T^2 \left(R^2 = 0.999\right)$$

$$\left(H - E/T\right) = 3.011 + 4.845T + 0.463T^2 \left(R^2 = 0.999\right)$$

$$\left(G - E/T\right) = -51.90 - 10.27T + 0.192T^2 \left(R^2 0.999\right)$$

All the thermodynamic data supply helpful information for the further study on the 3,5dHN2CA. They can be used to compute the other thermodynamic energies according to relationships of thermodynamic functions and estimate directions of chemical reactions according to the second law of thermodynamics in thermo chemical field.

Table 4. Second-order perturbation theory analysis of Fock matrix in NBO basic corresponding to the intra molecular bonds of 3, 5 dihydroxynaphthalene-2-carboxylicacid

Donor (i)	ED (i) (e)	Acceptor (j)	ED (j) (e)	[a]$E^{(2)}$ (kJ mol^{-1})	[b]E(j) – E(i) (a.u.)	[c]F(i,j) (a.u.)
σ(C_1–C_{19})	1.97350	σ*(C_2–C_3)	0.03248	4.51	1.08	0.062
σ(C_2–C_{20})	1.97320	σ *(C_{22}–H_{23})	0.01331	3.09	1.06	0.051
σ(C_3–O_{11})	1.99374	σ*(C_1–C_2)	0.01681	1.92	1.43	0.047
σ(C_5–O_{14})	1.99408	σ*(C_9–C_{10})	0.02865	1.77	1.39	0.045
σ(O_{11}–H_{12})	1.99170	σ*(C_3–C_4)	0.01700	3.21	1.36	0.059
σ(O_{14}–H_{15})	1.99010	σ*(C_5–C_{10})	0.02876	4.32	1.29	0.067
σ(C_{20}–O_{21})	1.99704	σ*(C_2–C_{20})	0.06862	0.91	1.43	0.046
σ(C_{20}–O_{22})	1.99591	π*(C_2–C_3)	0.03248	1.18	1.48	0.038
σ(O_{22}–H_{23})	1.98790	σ*(C_2–C_{20})	0.06862	4.14	1.13	0.062
LP(1)O_{11}	1.97902	σ*(C_2–C_3)	0.03248	6.24	1.07	0.073
LP(1)O_{14}	1.98191	σ*(C_5–C_6)	0.02033	4.94	1.20	0.069
LP(1)O_{21}	1.97215	σ*(C_2–C_{20})	0.06862	3.74	1.08	0.057
LP(1)O_{22}	1.97542	σ*(C_{20}–O_{21})	0.01853	6.82	1.16	0.079
LP(2)O_{11}	1.87671	π* (C_3–C_4)	0.29243	24.02	0.33	0.084
LP(2)O_{14}	1.89701	π* (C_5–C_6)	0.30543	22.15	0.35	0.083
LP(2)O_{22}	1.82532	π* (C_{20}–O_{21})	0.26173	45.56	0.33	0.112

[a] $E^{(2)}$ means energy of hyperconjugative interactions.
[b] Energy difference between donor and acceptor *i* and *j* NBO orbitals.
[c] *F(i,j)* is the Fock matrix element between *i* and *j* NBO orbitals.

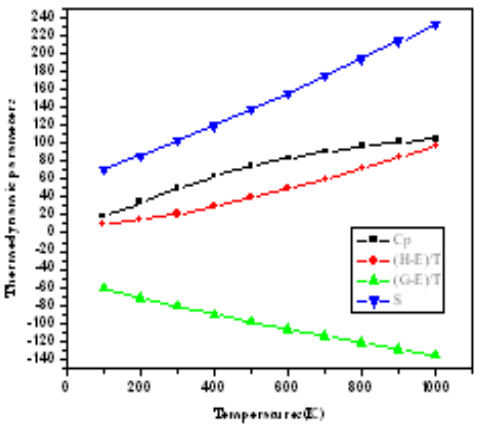

Fig 6. Correlation graphic of thermodynamic parameters and temperature for 3,5dihydroxynaphthalene-2-carboxylicacid

Notice: all thermodynamic calculations were done in gas phase and they could not be used in solution.

Table 5. Thermodynamic functions of 3, 5 dihydroxynaphthalene-2-carboxylicacid.

Temp (K)	Cp (Cal $Mol^{-1}K^{-1}$)	(H-E)/T (Cal $Mol^{-1}K^{-1}$)	(G-E)/T (Cal $Mol^{-1}K^{-1}$)	S (Cal $Mol^{-1}K^{-1}$)
100	18.549	9.303	-61.514	70.818
200	33.887	14.083	-72.091	86.175
300	49.468	20.915	-81.284	102.199
400	63.189	29.229	-89.998	119.226
500	74.405	38.699	-98.381	137.081
600	83.290	49.099	-106.449	155.548
700	90.331	60.254	-114.196	174.450
800	95.996	72.032	-121.619	193.651
900	100.635	84.324	-128.727	213.052
1000	104.495	97.046	-135.533	232.579

In addition to the vibrational assignments, several thermodynamic parameters, rotational constants, and dipole moment have been presented in Table 6. The self consistent field (SCF) energy, zero point vibrational energies (ZPVEs), rotational constants and entropy $S_{vib}(T)$ are calculated to the extent of accuracy and variations in the ZPVEs seem to be insignificant [38]. Dipole moment reflects the molecular charge distribution and is given as a vector in three dimensions. Therefore, it can be used as descriptor to depict the charge movement across the molecule. Direction of the dipole moment vector in a molecule depends on the centers of positive and negative charges. Dipole moments are strictly determined for neutral molecules. For charged systems, its value depends on the choice of origin and molecular orientation.

Table 6. Thermodynamic functions of 3,5 dihydroxynaphthalene-2-carboxylicacid.

Parametes	B3LYP/6-31+G(D)
Self consistent field energy	-724.9407 a.u
Zero point vibrational energy	107.431318(k.cal/mol)
Rotational constants	1.26186 GHz
	0.40070 GHz
	0.30413 GHz
Entropy	105.841 cal/mol-k
Specific heat capacity at constant volume	47.214 cal/mol-k
Translational energy	41.844cal/mol- K
Rotational energy	32.014 cal/mol-K
Vibrational energy	31.983 cal/mol-K

Conclusion

The molecular structure, vibrational spectrum, hyperpolarizability and NBO, HOMO–LUMO, MEP and thermodynamical analyses of 3,5dHN2CA are performed by density functional theory calculations. The equilibrium geometry by B3LYP/ccPVDZ and6-31+G(d) level for both the bond lengths bond angles and dihedral angles is performed better. On the basis of agreement between the calculated and experimental results, assignments of all the fundamental vibrational modes of 3,5dHN2CA are examined and proposed in this investigation. Comparison of the observed fundamental vibrational frequencies of 3,5dHN2CA and the results calculated by density functional B3LYP/ccPVDZ and 6-31+G(d) method indicates almost same approach for molecular vibrational problems. This is also confirmed by the natural bond orbital analysis. The lowering of HOMO–LUMO band gap supports bioactive property of the molecule.The MEP map shows that the negative potential sites are on electronegative atoms as well as the positive potential sites are around the hydrogen atoms. These sites give information about the region from where the compound can have intramolecular interactions. The thermodynamic features of the title compound at different temperatures have been calculated. It is seen that the heat capacities, entropies and enthalpies increase with theincreasing temperature owing to the intensities of the molecular vibrations increase with increasing temperature. In conclusion this study not only shows the way to the characterization of the molecule but also helps to researchers for the future studies in technology and industry.

References

[1] V. Krishnakumar, R. Mathammal, S. Muthunatesan, Spectrochim. Acta A 70 (2008) 201.
[2] M. Arivazhagan, V. Krishnakumar, G. John Xavier, V. Ilango, V. Balachandran, Spectrochim. Acta A 72 (2009) 941.
[3] D. Sajan, J. Binoy, B. Pradeep, K. Venkatakrishnan, V.B. Kartha, I.H. Joe, V.S. Jayakumar, Spectrochim. Acta A 60 (2004) 173.
[4] J.P. Abraham, I.H. Joe, V. George, O.F. Nielson, V.S. Jayakumar, Spectrochim. Acta A 59 (2003) 193.
[5] J. Binoy, J.P. Abraham, I.H. Joe, V.S. Jayakumar, J. Aubard, O.F. Nielson, J. Raman Spectrosc. 36 (2005) 63.
[6] M.J. Frisch, G.W.Trucks, H.B. Schlegal, G.E. Scuseria, M.A. Robb, et al., Gaussian 09, Revision A. 02, Gaussian Inc., Wallingford, CT, 2009.
[7] A. Frisch, A.B. Niesen, A.J. Holder, Gauses View Users Manual, Gaussian Inc.,2008.
[8] M. Silverstein, G.Clayton Basseler, C. Morill, Spectrometric Identification of Organic Compound, Wiley, New York, 1981.2560.
[9] J. Coates, R.A. Meyers (Eds.), Interpretation of Infrared Spectra: A Practical Approach, John Wiley and Sons Ltd., Chichester, 2000.
[10] V. Balachandran, V. Karpagam, J. Mol. Struct. 1038 (2013) 52–61.
[11] M. Silverstein, G.C. Basseler, C. Morill, Spectrometric Identification of Organic Compounds, Wiley, New York, 1981.
[12] P.S. Kalsi, Spectroscopy of Organic Compounds, Wiley Eastern Limited, New Delhi, 1993. p. 116.
[13] D.N. Sathyanarayana, Vibrational Spectroscopy – Theory and Applications, second ed., New Age International (P) Ltd. Publishers, New Delhi, 2004.
[14] G. Socrates, Infrared and Raman Characteristic Frequencies, third ed., John Wiley & Sons Ltd., Chichester, 2001.
[15] V.R. Dani, Organic Spectroscopy, Tata – MacGraw Hill Publishing Company, New Delhi, 1995. pp. 139.
[16] N.B. Clothup, L.H. Daly, S.E. Wiberley, Introduction to Infrared and Raman Spectroscopy, Academic Press, New York, 1990.
[17] V. Krishnakumar, V. Balachandran, Indian J. Pure Appl. Phys. 47 (2009) 823–827.
[18] H.J. Singh, P. Srivastava, Indian J. Pure Appl. Phys. 47 (2009) 557–562.
[19] J. Mohan, Organic Spectroscopy – Principle and Applications, second ed., Narosa Publishing House, New Delhi, 2001.
[20] D. Lin-Vein, N.B. Colthup, W.G. Fateley, J.G. Grasselli, The Handbook of Infrared and Raman Characteristic Frequencies of Organic Molecules, Academic Press, San Diego, 1991.
[21] C.B. Smith, Infrared Spectral Interpretation, CRC Press, New York, 1999.

[22] J. Coates, Interpretation of infrared spectra a practical approach, in: R.A. Meyers (Ed.), Encyclopedia of Analytical Chemistry, John Wiley & Sons Ltd., Chichester, 2000.
[23] P. Venkoji, Indian J. Pure Appl. Phys. 24 (1986) 166.
[24] J. Marshal, Indian J. Phys. 72B (1998) 661.
[25] S. Ahamed, S. Mathew, P.K. Verma, Ind. J. Phys. 30 (1992) 764.
[26] S. Ahmad Siddiqui, A. Dwivedi, N. Misra, N. Sundaraganasan, J. Mol. Struct.(Theochem) 827 (2007) 101–106.
[27] C. James, A. Amal Raj, R. Rehunathan, I. Hubert Joe, V.S. Jayakumar, J. Raman Spectrosc. 37 (2006) 1381–1392.
[28] Liu Jun-na, Chen Zhi-rong, Yuan shen-feng, J. Zhejiang University Sci. B 6 (2005) 584.
[29] S. Sebastian, N. Sundaraganesan, Spectrochim. Acta A 75 (2010) 941–952.
[30] B.J. Powell, T. Baruah, N. Bernstein, K. Brake, R.H. McKenzie, P. Meredith, M.R. Pederson, J. Chem. Phys. 120 (2004) 8608–8615.
[31] T. Vijayakumar, I. Hubert Joe, C.P.R. Nair, V.S. Jayakumar, J. Chem. Phys. 343 (2008) 83–99.
[32] Xavier Assfeld, J.L. Rivail, Chem. Phys. Lett. 263 (1996) 100–106.
[33] R.S. Mulliken, J. Chem. Phys. 23 (1955) 1833–1841.
[34] A.E. Reed, F.J. Weinhold, L.A. Curtiss, Chem. Rev. 88 (1988) 899–926.
[35] R.G.Parr, L.V. Szentpaly, S.J. Liu, Am. Chem. Soc. 121 (1999) 1922–1924.
[36] P.Politzer,J.S.Murray,Theoretical biochemistry and molecular biophysics: a comprehensive survey, in: D.L. Beveridge, R. Lavery (Eds.), Electrostatic Potential Analysis of Dibenzo-p-dioxins and Structurally Similar Systems in Relation to their Biological Activities, Protein, vol. 2, Academic Press, Schenectady, NY, 1991 (Chapter 13).
[37] P. Politzer, J. Murray, Theor. Chem. Acc. 108 (2002) 134–142.
[38]. P.B.Nagabalasubramanian, S. Periyandi, S. Mohan, Spectrochim. Acta, Part A 77 (2010) 150–159.